BILINGUAL PUBLISHING GROUP

Journal of Environmental & Earth Sciences

https://journals.bilpubgroup.com/index.php/jees

ARTICLE

Hydrogeochemical Processes in Basement Areas Using Principal Component in Burkina Faso (West African Sahel)

Moussa Diagne Faye [1*] **, *Vini Yves Bernadin Loyara*** [2] **, *Amadou Keita*** [1] **, *Mamadou Diop*** [3]**, *Angelbert Chabi Biaou*** [1]**, *Mahamadou Koita*** [1]**, *Hamma Yacouba*** [1]

[1] *Laboratory of Water, Hydro-Systems and Agriculture (LEHSA), International Institute for Water and Environmental Engineering (2iE), Ouagadougou P.O. Box 594, 01, Burkina Faso*

[2] *Laboratory of Numerical Analysis of Computer Science and Biomathematics (LANIBIO), Joseph KI-ZERBO University, Kaya Polytechnic University Center, Kaya P.O. Box 232, Burkina Faso*

[3] *Eco-Materials and Sustainable Habitats Laboratory (LEMHaD), International Institute for Water and Environmental Engineering (2iE), Ouagadougou P.O. Box 594, 01, Burkina Faso*

ABSTRACT

The basement aquifers in Burkina Faso are increasingly exposed to groundwater pollution, largely due to socio-economic activities and climatic fluctuations, particularly the reduction in rainfall. This pollution makes the management and understanding of these aquifers particularly complex. To elucidate the processes controlling this contamination, a methodological approach combining principal component analysis (PCA) and multivariate statistical techniques was adopted. The study analyzed sixteen physicochemical parameters from 58 water samples. The primary objective of this research is to assess groundwater quality and deepen the understanding of the key factors influencing the spatial variation of their chemical composition. The results obtained will contribute to better planning of preservation and sustainable management measures for water resources in Burkina Faso. The results show that three principal components explain 72% of the variance, identifying anthropogenic inputs, with two components affected by mineralization and one by pollution. The study reveals that the groundwater is aggressive and highly corrosive, with calcite saturation. Water-rock interactions

*CORRESPONDING AUTHOR:

Moussa Diagne Faye, Laboratory of Water, Hydro-Systems and Agriculture (LEHSA), International Institute for Water and Environmental Engineering (2iE), Ouagadougou P.O. Box 594, 01, Burkina Faso; Email: moussa.faye@2ie-edu.org

ARTICLE INFO

Received: 23 July 2024 | Revised: 13 August 2024 | Accepted: 2 September 2024 | Published Online: 28 October 2024
DOI: https://doi.org/10.30564/jees.v7i1.6932

CITATION

Faye, M.D., Loyara, V.Y.B., Keita, A., et al., 2024. Hydrogeochemical Processes in Basement Areas Using Principal Component in Burkina Faso (West African Sahel). Journal of Environmental & Earth Sciences. 7(1): 1–17. DOI: https://doi.org/10.30564/jees.v7i1.6932

appear to be the main mechanisms controlling the hydrochemistry of groundwater, with increasing concentrations of cations and anions as the water travels through percolation pathways. PCA also revealed that the residence time of the water and leaching due to human activities significantly influence water quality, primarily through mineralization processes. These results suggest that rock weathering, coupled with reduced rainfall, constitutes a major vulnerability for aquifer recharge.
Keywords: Groundwater; Hydrogeochemistry; Spatial Analysis; Principal Component Analysis

1. Introduction

Groundwater, a vital resource for humanity, is facing increasing challenges due to various factors such as climate change, organic and inorganic contamination, and salinization. These threats have significantly degraded the quality of this resource, making its management and conservation increasingly complex. The accumulated groundwater contamination, largely due to the expansion of anthropogenic activities such as intensive agriculture, rapid urbanization, and mining, demands particular attention[1–8]. Exploitation through boreholes, which mainly tap into aquifers altered by mineralogical weathering, exposes these resources to additional risks[9–12]. It is therefore essential to evaluate future trends in water quality to ensure effective and sustainable groundwater management.

Climate change, for example, not only affects the availability of water resources but also their quality by exacerbating phenomena such as salinization and the introduction of new or re-emerging contaminants. Furthermore, inadequate management of industrial and agricultural waste leads to the accumulation of organic and inorganic contaminants, such as nitrates and heavy metals, in aquifers, further worsening groundwater pollution problems.

In this context, several approaches have been proposed to address these issues using methods adapted to local conditions. For instance, Noronha et al.[13] in Portugal developed a three-step fluid flow model for metallogenesis, while researchers in Nigeria[14–18] focused on abandoned waste sites or dumps. Other studies, such as that by Penant[19] in Benin, have focused on nitrate contamination sources, with similar research conducted in Morocco[20], in England[21] and in Burkina Faso[22]. Despite these efforts, the periodic monitoring of water points remains insufficient, exposing populations to risks associated with poor-quality drinking water.

In Burkina Faso, groundwater is particularly vulnerable to pollution, making hydrochemical studies more difficult and complex. The increasing contamination, still poorly understood, coincides with a growing demand for water, exacerbated by changes in land use, notably the expansion of industrial mining activities and the adoption of chemically intensive agriculture. In 2015, for instance, 40% of boreholes were closed or abandoned due to high arsenic levels, underscoring the urgency of better water resource management[23–25]. This situation is further compounded by a shift in land use within municipalities, with 57.84% attributed to the rise in industrial mining activities and a shift toward chemically intensive agriculture, representing 85% of the sampled sites.

In the face of these challenges, it is crucial to understand the hydrogeochemical processes governing groundwater quality in these complex environments. This research aims to determine the sources and extent of groundwater contamination to deepen our understanding of the parameters controlling the spatial variation of chemical transfer. To achieve this, we will employ Principal Component Analysis (PCA) and other multivariate statistical techniques.

The PCA method, widely used in geochemistry, allows for the interpretation of complex data matrices involving multiple variables[26–33]. It provides an effective visualization of the data by grouping different chemical species according to their origin, thus simplifying the complexity of the matrix[34–36]. Consequently, PCA helps to explore geochemical data by condensing them into a new set called principal components, which facilitates a better understanding and management of issues related to groundwater quality[32, 37–39]. The PCA plot represents the coordinates of variances, allowing for the exploration of geochemical data (multivariable data). Therefore, we consider variables as different projections based on their affinities or characteristics. PCA enables the extraction and visualization of the essence of the data, reducing or condensing the data into a new dataset called principal components, derived from the original data. The

number of principal components is never greater than the number of original variables [40].

2. Materials and Methods

2.1. Study Area

The study site is in the Sahelo-Sudanian zone in West Africa, with GPS coordinates of 11° and 12° N and 1° 48′ ; 2° 24′ W. The territory is divided into several watersheds, including the study area covering an area of 7500 km^2 (**Figure 1a**). It is crossed by the Sissili River, which rises in the basin and flows southwards, ending in the Tô department. It covers entirely or partially 12 communes, namely Thyou, Bougnounou, Dalo, Bakata, Cassou, Gao, To, Sapouy, Leo, Bieha, Guiaro, Po, and 3 provinces, namely Boulkiemdé, Sissili, and Nahouri.

The population is estimated at 20,505,155 inhabitants, with 8,217,864 inhabitants in the study area. It comprises around sixty ethnic groups, with an annual growth rate ranging from 4.42% to 2.6%. The population density is estimated at 100 inhabitants per km^2. In rural areas, water supply is provided in the study area through modern wells (90.9% in 2021) and AEPS (87.1% in 2021). The national access rate is 76.2% in 2021. This implies high demand from the population, leading to the utilization of natural resources.

We mainly encounter agricultural areas, which dominate in terms of coverage, and wetlands. The soil distribution between 2012 and 2018 shows that a majority proportion of the total area, 57.84%, is now occupied by agricultural zones [25] (**Table 1**).

Water resources are heavily dependent on the type of climate and climatic parameters, mainly precipitation, temperatures, air humidity, winds, evapotranspiration, and evaporation. Rainwater runoff constitutes the main source of supply for surface water capture structures, while infiltration and groundwater flow are the main vectors for aquifer replenishment. The climate has two distinct periods. The climate is Sudanian (southern Sudanian).

The hydrological station of the Sissili in Kounou was established in 1965 and provides information on the volume for the period 1965–2012, which is 2.81 million m^3, while the average interannual flow rate is 2.81 m^3 s^{-1}. Regarding geology (**Figure 1b**), the watershed exhibits two main Proterozoic geological units and sedimentary [41, 42]. However, three types of geological formations can be distinguished as particularly productive.

Conversely, volcanic sedimentary formations generally exhibit lower hydraulic productivity, allowing flows greater than 5 m^3 h^{-1}. For post-tectonic intrusive plutons, the flow rates are barely above 5 m^3 h^{-1} and can drop to 2 m^3 h^{-1} [1].

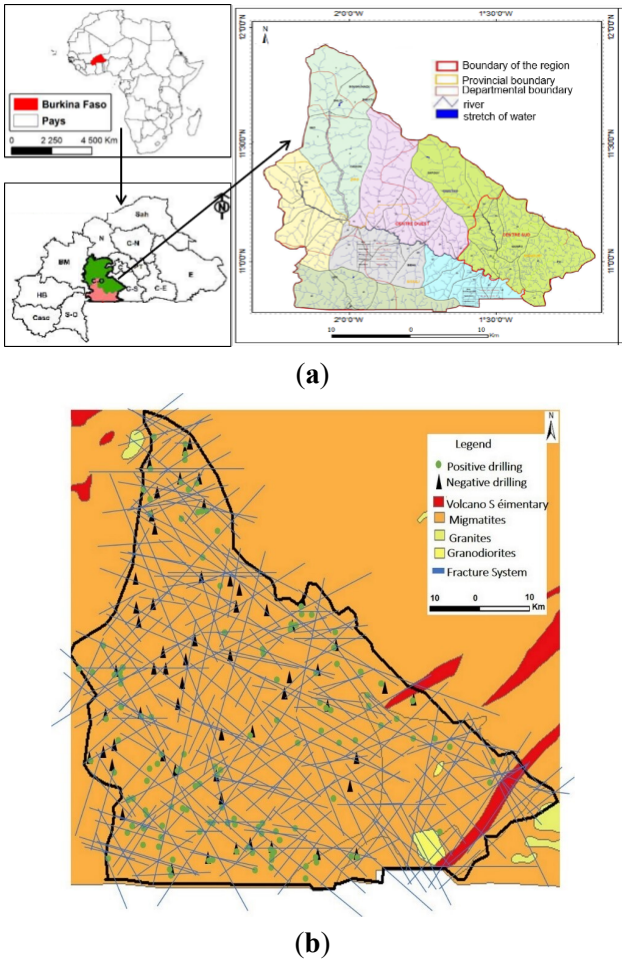

Figure 1. (**a**) Localization of the study zone of study. (**b**) Geological map overlaid with boreholes [10].

2.2. Groundwater Data Sampling and Analytical Method

The Burkinabé government, in its effort to improve access to water for the rural population, regularly initiates campaigns to monitor water quality and assess pollution risks related to water resources in 13 regions. The 2012 analysis campaign revealed high levels of certain chemical parameters in the sub-basin that could affect water quality. Indeed, it highlighted harmful chemical elements in significant concentrations in the water of certain localities. Addition-

Table 1. Land cover matrix from 2002 to 2018 [25].

Units	Fields	Riparian Formation	Habitat	Body of Water	Sanave with Trees	Shrubby Savannah	Bare/ Eroded Area	Total 2018
Fields	**71946.93**	1800.92	598.87	23.40	43498.14	66557.16	2530.89	186956.32
Riparian formation	78.30	**650.37**	10.80	2.34	1826.92	830.56	31.17	3430.46
Habitat	780.77	40.69	**279.29**	1.26	166.29	320.29	7.74	1596.32
Body of water	39.51	11.95	6.66	**47.52**	136.59	68.02	4.34	314.59
Sanave with trees	6811.71	1757.92	131.29	1.71	**18219.22**	18379.22	707.17	46008.25
Shrubby savannah	4812.79	2461.89	262.79	1.17	27788.81	**42228.20**	1768.92	79324.59
Bare/eroded area	213.40	367.18	1.71	0.00	1511.94	3012.87	**476.38**	5583.47
Total 2002	84683.40	7090.94	1291.41	77.40	93147.93	131396.31	5526.61	323214.00

ally, highly mineralized waters were also identified, which could pose kidney problems for the population. Sampling was conducted on 58 water samples in accordance with standard norm recommendations (**Figure 1**) [43–45]. The sampling methodology developed involved a grid of 10 square kilometers covering the regions. In each grid cell, we collected 8 samples to cover all geological formations present per cell.

For our case, 16 parameters were analyzed using data processing, although the method relys on existing methods. T°, pH, and EC were measured by multiparameter device. NO_3^-, SO_4^{2-}, NO_{2^-}, $PO4_3^-$, Fe^{2+}, NH_4^+, and F^- were measured by molecular absorption spectrophotometry. Na^+ and K^+ were measured by flame atomic emission photometry. The method used to evaluate total cyanide involved spectrophotometry. As, Pb, and Zn were detected using microwave plasma atomic emission spectrometry. CO_3^{2-}, HCO_3^-, and Cl^- were performed using volumetric methods with sulfuric acid and silver nitrate, respectively.

Some physicochemical variables are missing or contain input errors (use of dot and comma as decimal separator, negative value). Therefore, our first step is to correct the input data. To do this, we will start with the linear regression method. This analysis involves making a correlation, calculating the mean and mode of the already corrected data. Then, statistical analysis (correlation, mean) will complement the missing data. Through the correlation matrix, we can see which data correlate best. This gap-filling method is based on the principle that data closer to each other are more similar compared to data located at a greater distance where the geology may differ, for example.

Still aiming to correct the missing data, we will also use the ion balance (Equations (1) and (2)). This is justified here because in drilling installations, many ions are often not considered. Some authors define the acceptable margin of error for ion balance equilibrium (IBE) as ±5% [7] while others set it at ±10% [44, 46]. The range of ±5% has been provided for discrepancies and strengthens the analyses [3].

$$[Cl^-] + [SO_4^{2-}] + [NO_3^-] + [HCO_3^-] = [Ca^{2+}] + [Mg^{2+}] + [Na^+] + [K^+] \quad (1)$$

$$\text{The error percentage is given by} : IBE = \frac{\sum cations - \sum anions}{\sum cations + \sum anions} * 100 \quad (2)$$

2.3. Multivariate Analysis

The method implemented for the mineralization of water relies on principal component analysis. Choosing a data analysis technique agrees for easy extraction of important information in its raw state.

To assess the consistency of the variables, we used the Kaiser-Meyer-Olkin measure and Bartlett's test of sphericity to determine if there was a difference. These methods have been widely employed to analyze groundwater samples as well as physico-chemical variables.

The literature has assisted in selecting an appropriate data mining method based on the type of problem:

- Exploratory approaches facilitate the exploration of multivariate datasets without the need to confirm a specific

hypothesis. Exploratory analysis techniques often involve reducing voluminous data to make their exploration easier.

- Decision-making issues involve testing the relationship between two groups of variables (correlation) or explaining one variable or group of variables by another group (causality).

In this study, a correlation analysis will be used, where a correlation indicates a strong relationship if it is close to 1; this will help to understand their reciprocal relationships [28, 47].

2.4. Acquisition and Mineralization Processes of Groundwater

This approach involved, in the case of our study, determining the saturation indices (SI) and the Ryznar indices (RSI) of certain minerals present in the bedrock zone using the PHREEQC module of the Diagrammes software. Based on the content of the main chemical elements, Yameogo [48] mentions that the water balance can be determined, contributing to the understanding of water properties and behaviors, such as their tendency to be corrosive or to form deposits. The saturation index is determined by the product of ionic activity. The saturation index (SI), expressed by Equation (3), measures the deviation from equilibrium:

$$IS = \log(PAI) – \log(T) \quad (3)$$

The lack of drilling technical sheets has limited the distinction between waters from the weathered aquifer and the fractured zone or coarse sand aquifers. Additionally, due to the imprecision in the calculations, Kouanda et al. [46] and Moussa, Zouari and Marc [49] propose considering saturation to be achieved within a slightly wider range such as $-1 < SI < 1$. Furthermore, it is recommended to use various bivariate diagrams for further investigation into the sources of demineralization of waters.

The Ryznar index is determined by the empirical formula, which is written as follows in Equation (4):

$$pHs = (9.3 + A + B) - (C + D) \quad (4)$$

2.5. Principal Component Analysis (PCA)

The statistical analysis was performed by R code. A dataset's total variance or inertia is represented. The goal is to find the axes along which the data exhibit the greatest variation. By reducing the dimensions of multivariate data, PCA typically represents them as axes, while retaining as many necessary elements [29, 50–53].

2.6. Factor Transformation

The fundamental problem that PCA addresses is to convert a group of correlated variables into independent variables. Under ideal conditions, these new variables can be viewed as underlying factors. That's is why these orthogonal quantities are called "factors", although this interpretation may not always be perfectly accurate [51, 54, 55].

Z is the matrix n × n data-centric data and V is the corresponding variance-covariance matrix n × n as shown in Equation (5):

$$V = [\sigma_{ij}] = \frac{1}{n} Z^{T} z \quad (5)$$

y is a matrix n × n corresponding to n samples of uncorrelated factors y_p, $p \in \{1,...,n\}$ and with no expectations, as shown in Equation (6):

$$D = \frac{1}{n} y^{T} y \quad (6)$$

We are searching for an orthogonal matrix A, of size N × N, to make them into synthetic factors Equation (7).

$$y = ZA \text{ avec } A^{T}A = I \quad (7)$$

To make them into synthetic factors, we need to add the term $\frac{1}{n}$ and by y^{T} on a in Equation (8):

$$\frac{1}{n} y^{T} y = \frac{1}{n} Z^{T} zA \quad (8)$$

2.7. Maximizing the Variance of a Factor

PCA allows capturing the maximum portion of the variance of the variables [52]. Let's consider (Equation (9)) obtained by extracting the variables from Z using a calibrated unit vector a_1.

$$y_1 = Za_1 \text{ avec } {a_1}^{T} a_1 = 1 \quad (9)$$

To allocate a maximum portion of the variance y_1, it is necessary to identify an objective function $\varnothing_1$, adopting λ_1, thereby adding a unit norm constraint to the vector a_1 [53] Equation (10):

$$\varnothing_1 = {a_1}^{T} V {a_1}^{T} - \lambda_1 ({a_1}^{T} a_1 - 1) \quad (10)$$

Next, y_2 added as another vector orthogonal to the first one Equation (11):

$$\mathrm{Cov}(y_2, y_1) = \mathrm{Cov}(Za_1, Za_2) = a_2{}^{T}Va_1{}^{T} = a_2{}^{T}\lambda_1 a_2 = 0 \quad (11)$$

$\varnothing_2$ to be maximized contains the choice of a_2 normalized to unity, and a_2 with a_1, thereby adding a unit norm constraint to λ_2 and μ Equation (12).

$$\varnothing_2 = a_2{}^{T}Va_2{}^{T} - \lambda_2(a_2{}^{T}a_2 - 1) + \mu a_2{}^{T}a_1 \quad (12)$$

By adding $a_1{}^{T}$, the value μ is shown by the Equation (13):

$$\mathrm{Tr}\,(V) = \sum_{i=0}^{n} \sigma ii = \sum_{i=0}^{n} bi \quad (13)$$

2.8. Interpretation of Factor Variances

Equation (14) characterizes the portion of the total variance usually given as a percentage

$$\frac{Variance\ of\ te\ factor}{Total\ variance} = \frac{\lambda p}{Tr\,(V)} \quad (14)$$

It is considered that if an identity is below 1, it is accepted that the factor defining the value is less than the measured value because its variance is less than the unit variance of the variables [56, 57].

2.9. Correlation of Variables with Factors

We work with standardized data $\widetilde{Z}\alpha i$ to bring all variables to the same scale (Equation (15)):

$$\widetilde{Z}_{\alpha_i} = \frac{z\alpha i - mi}{\sqrt{\sigma ii}} \quad (15)$$

where mi and $\sqrt{\sigma ii}$ are the mean and standard deviation of the variable z_i. The correlation matrix is represented in Equation (16):

$$R = \frac{1}{n}\widetilde{Z}^{T}\widetilde{Z} \quad (16)$$

The length of vectors a_i is equal to one (Equation (17)):

$$a_i{}^{T}a_j = \rho_{ij} \quad (17)$$

From a geometric perspective, the vectors a_i position ρ_{ij} as the cosines of the angles between two vectors corresponding to different variables [56, 57].

The projection of variable positions from the surface of the hypersphere onto planes defined by factorial axes provides a graphical representation known as a "correlation circle", showing their proximity within an originally centered unit circle. These representations are useful for assessing the affinity or antagonism between variables. These plots are reliable if the variables of interest are centered around the circle. Otherwise, multiple factorial planes must be examined to ensure that observed proximity on one circle corresponds to proximity on the hypersphere [29].

We can also create correlation circles between the variables and pairs of factors. We multiply the V matrix on the left and right by the diagonal matrix of inverse standard deviations (Equation (18)):

$$\mathrm{Corr}(z_i, y_p) = \sqrt{\frac{\lambda p}{\sigma ii}}\, q_{ip} \quad (18)$$

3. Results and Discussion

3.1. Subsection Groundwater Analysis

The study area is divided among 13 municipalities, which do not have the same geological contexts. Linear regression curves were used to assess the quality of correlations (**Figure 2**). They allowed us to fill in the missing values relative to the input values. The equation of EC as a function of TDS determined the line y = 0.8428x + 12.215. TDS, like EC, describes the inorganic salts present in water solution with a correlation (R^2 = 0.74). TAC is mainly due to HCO_3, ranging from 5 mg L^{-1} and reflects the low values of bicarbonate ions compared to TDS (**Figure 2**) with a correlation of (R^2 = 0.56) and a line y = 0.4367x + 46.311. The explanation we can give is that a large number of variables makes it difficult to correlate a certain number of explanatory variables. These variables generate lower standard errors than the constant. However, reducing the number is necessary for clarity.

The ion balance in the samples varies from 0% in Kayabo to 31% in Boala. Finally, ion balance is verified based on the levels of measured ions (<10%), considering certain high ionic charges. However, not all samples have a balanced ion balance. The samples from Boala, Métio, and Kayero-bo are not reliable (>10%), but they appear low in terms of the results. The waters of these three villages could be dominated by trace metal elements. These traces are not considered when calculating the balance. This discrepancy may also arise from invalid analysis results or ions present in the water that have not been analyzed. The presence of all major elements is also noted in the various samples. This

could result from a lack of precision in the analysis methods used. The results show that samples with a balanced balance have better values for comparison criteria[7, 26]. Thus, based on these results, ion balance is therefore reliable for the treatment of physico-chemical data of groundwater. This was supported by linear regression.

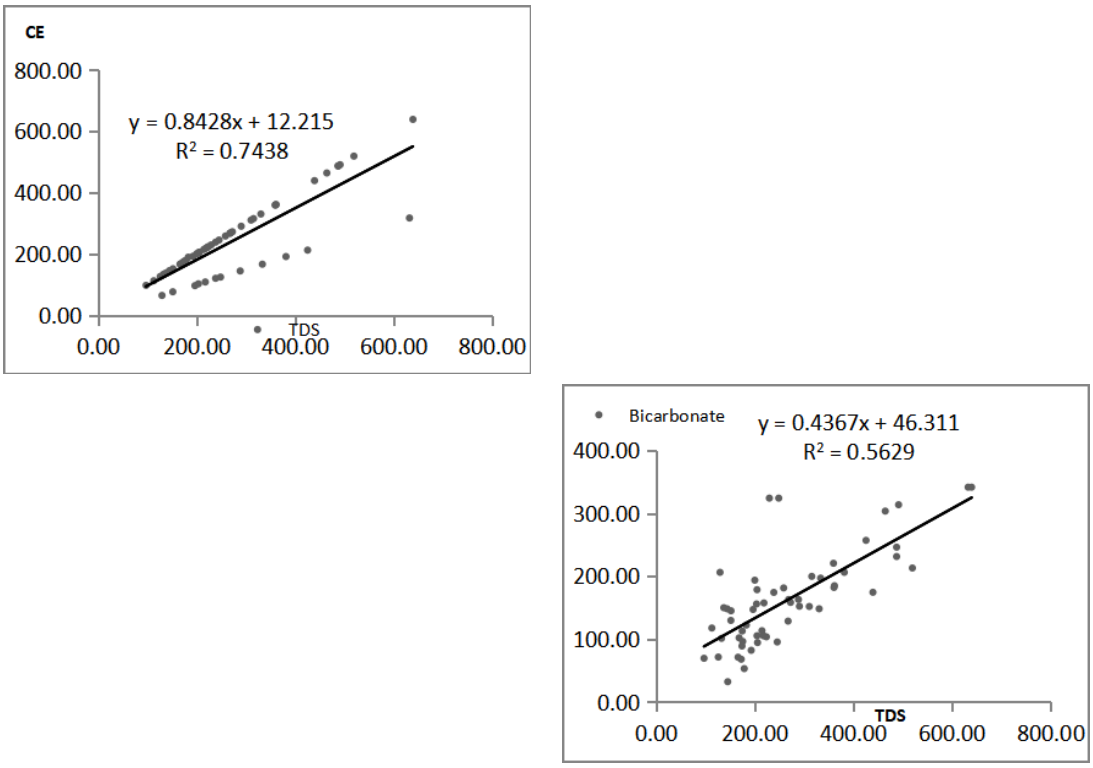

Figure 2. Linear regression between parameters, HCO_3 and TDS; TDS and EC in groundwater.

3.2. Water Quality Data Processing and Analysis

3.2.1. Multivariate Analysis of Different Physicochemical and Chemical Variables

The reduction of information is to a small number. It is therefore a method that is both exhaustive and truthful (representation of variables in a space according to directions of maximum inertia) (**Figure 3** and **Table 2**).

Significant links are reflected in the various correlations. We observe a moderate to strong correlation of HCO_3^- ions with Ca^{2+} ($R^2 = 0.61$), Mg^{2+} ($R^2 = 0.79$), Na^+ ($R^2 = 0.60$), K^+ ($R^2 = 0.51$), as well as with NH_4^+ and iron ($R^2 = 0.87$), due to the alteration of silicates. When soluble elements are leached, we observe a recombination with other ions, or they remain static. Infiltration waters contain CO_2, and this CO_2 rich water can corrode aluminosilicate minerals such as plagioclase and biotite in rocks[48]. The partially crystallized intermediate phases reassemble into neoformed materials, particularly clays. This is confirmed by (**Figure 5**), as most groundwater reaches chalcedony, calcite, and dolomite saturation but is undersaturated in halite and gypsum.

The relationships between cation concentrations and HCO_3^- in the bedrock environment suggest that the alteration of silicates may be due to other factors. PCA shows this well, indicating that K and Na result from strong anthropogenic pressure. It can be noted that the dominant process is the dissolution of limestone minerals under the influence of carbon dioxide. With the fault being open, biogenic carbon dioxide spreads very easily at the level of shallow piezometers during recharge. There is no pronounced dominance for Na and K; however, for magnesium, this is due to anthropogenic input.

The relationships between cation concentrations and Cl^- show no correlation between these parameters (Ca^{2+}) ($R^2 = 0.27$), (Na^+) ($R^2 = 0.29$), (Mg^{2+}) ($R^2 = 0.36$), (K^+) ($R^2 = 0.47$), except Na and K. It should be noted that Na^+

and K^+ increase as Cl^- concentrations decrease, suggesting that the concentration levels appear to be independent or have different sources in the sub-basin. This is explained by the absence of minerals containing a high chloride content in the rocks, which is included in biotite[12, 58, 59]. For Mg, we observe the least mineralized waters, which suggests an external input.

The relationships between anion concentrations and Cl^- are almost non-existent: HCO_3^- ($R^2 = 0.40$), NO_3^- ($R^2 = 0.34$), SO_4^{2-} ($R^2 = 0.33$). Bicarbonate ions do not show a clear correlation with chlorides, suggesting chlorides in the water are probably not due to silicate weathering. There is an association or clustering in the relationship between nitrates and chlorides. We observe that three wells with high nitrate concentrations stand out in the villages of Koumbogoro in the Bieha commune and Don in the Leo commune. This suggests a likely common anthropogenic origin (related to agriculture), indicated by the fact that these wells are located in agricultural areas, as indicated by land use. High chloride levels do not accompany high nitrate levels. This disparity may be due to the presence or absence of denitrification in the pollution source. Regarding the relationship between orthophosphates and chlorides, as well as between sulfates and chlorides, two distinct trends are observed. Extreme values could be attributed to domestic pollution sources from nitrates or chemical fertilizers used in fields.

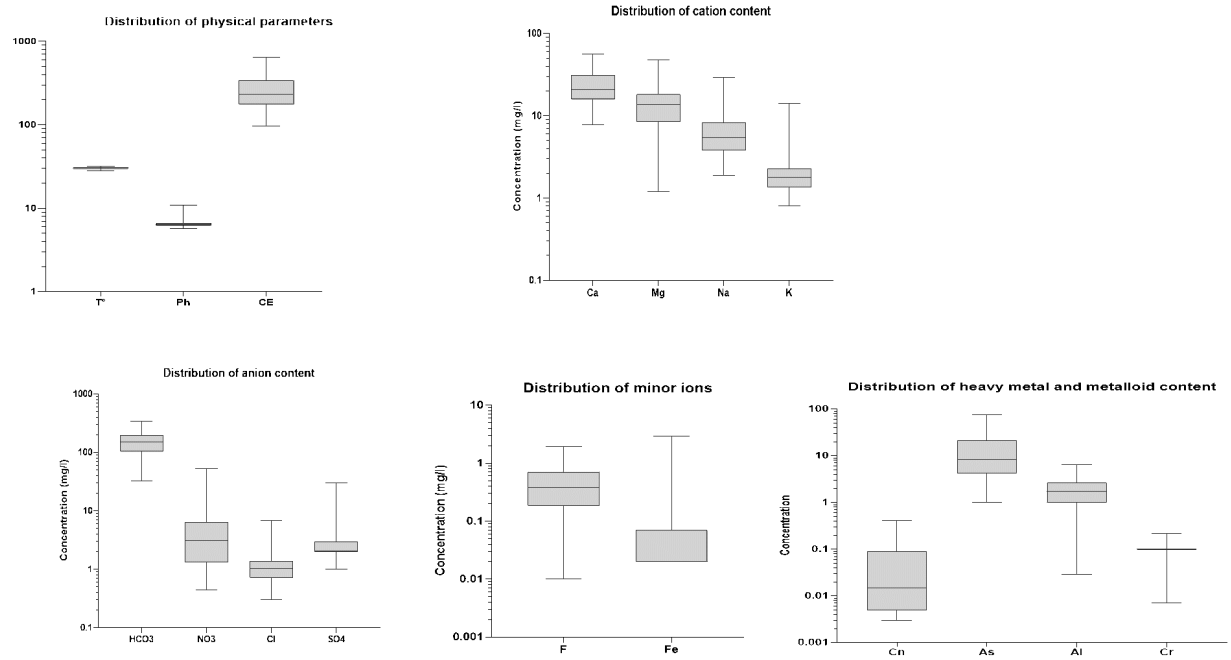

Figure 3. Box plot of the distribution of physicochemical parameters.

3.2.2. Groundwater Acquisition and Mineralization Process

Figure 4 shows the statistical parameters of saturation indices (IS < −1) undersaturation relative to calcite. Undersaturation with respect to calcite, aragonite, gypsum, and anhydrite is noted. The values that exceed the norm for calcite and frequent interaction between water and rock in the wells tend to elevate the pH, IS is equilibrium. Conversely, gypsum and anhydrite exhibit a favorable equilibrium state for dissolution in water. For dolomite (**Figure 5a**) and calcite, a dominance of samples in a state of oversaturation is observed, and an equilibrium state with respect to carbonate minerals (−1 < IS < 1) is also observed for some samples. There is a dominance of Ca^{2+} over SO_4^- in all samples (**Figure 5b**), which may indicate that gypsum and anhydrite dissolution is obviously a secondary process and that other reactions have occurred and contributed significantly to the production of Ca^{2+} ions relative to SO_4^- in the different aquifers. This is supported by the predominance of the calcic and magnesian bicarbonate facies. A common origin of Ca,

Table 2. Groundwater correlation matrix.

	Ca^{2+}	Mg^{2+}	Na^{+}	K^{+}	Fe^{2+}	NH_4^{+}	Cl^{-}	SO_4^{2-}	NO_3^{-}	NO_2^{-}	POs4^{-}	P	F	Al	As	Zn	HCO_3^{-}
Ca^{2+}	1																
Mg^{2+}	0.26	1															
Na^{+}	0.43	0.37	1														
K^{+}	0.3	0.46	**0.64**	1													
Fe^{2+}	0.02	−0.04	−0.19	−0.03	1												
NH_4^{+}	−0.01	−0.02	−0.14	0	**0.87**	1											
Cl^{-}	0.27	0.36	0.29	0.47	0.13	0.19	1										
SO_4^{2-}	**0.59**	0.26	0.4	0.41	−0.04	−0.04	0.33	1									
NO_3^{-}	0.08	0.47	0.35	**0.62**	0.16	0.07	0.34	0.26	1								
NO_2^{-}	0.17	0.42	0.39	**0.5**	0.03	−0.03	0.24	0.2	**0.63**	1							
POs4^{-}	−0.1	−0.14	0.02	−0.11	−0.14	−0.15	−0.28	−0.23	−0.25	−0.17	1						
P	−0,1	−0,14	0.02	−0.11	−0.14	−0.15	−0.28	−0.23	−0.25	−0.17	**1**	1					
F	0.28	0.13	0.43	0.13	−0.16	−0.19	−0.04	0.29	0.06	−0.05	0.02	0.02	1				
Al	−0,15	−0.1	0.13	0.06	−0.18	−0.19	−0.16	−0.13	0.01	−0.02	0.37	0.37	0.04	1			
As	−0,05	−0.28	−0.3	−0.21	0.04	−0.08	−0.12	0.1	−0.12	−0.05	−0,18	−0.18	0.15	−0.26	1		
Zn	0.15	0.15	−0.13	0.01	0.07	0.04	0.01	−0.07	0.33	0.07	−0.11	−0.11	−0.05	0.06	−0.13	1	
HCO_3^{-}	**0.61**	**0.79**	**0.6**	**0.52**	−0.05	−0.01	0.4	0.44	0.33	0.31	−0.11	−0.11	0.25	−0.1	−0.32	0.02	1

Mg, and HCO_3 minerals confirms dolomite dissolution. It was concluded that the saturation index does not allow for understanding the geochemical mechanism of demineralization. Because generally, no formation of carbonate minerals, such as calcite, is detected in the granitic basement rocks. It is clear that the dissolution of calcium aluminosilicate minerals by dissolved carbon dioxide in water constitutes the primary process influencing mineral acquisition and progression. The absence of correlation between Na and Cl^{-} anthropogenic input confirms halite dissolution (**Figure 5c**). These results conclude that IS does not allow understanding the mechanism of water demineralization from the absence of calcite precipitations in rocks.

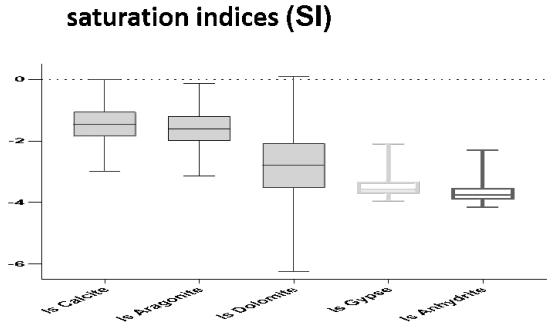

Figure 4. Statistical parameters of saturation indices.

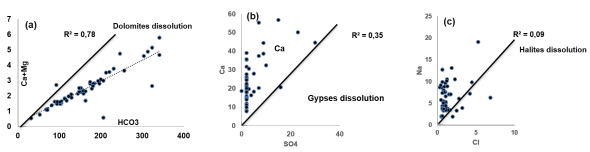

Figure 5. Dissolution line: (**a**) dolomites, (**b**) gypses and (**c**) halites.

Figure 6 shows the statistical parameters of Ryznar (RSI) RSI > 7 aggressive and highly corrosive waters. It helps to define an aggressive (corrosive) trend of the water. The trend indicates aggressive and highly corrosive waters, except for the Yaké borehole in the To municipality, which has an incrusting water that will lead to calcium carbonate deposition. In various studies, it has been demonstrated that water can be corrosive in acidic rocks such as granite and schist. Conversely, when the rock is basic, when the pH is above 7, such as basalt and dolerite, water tends not to exhibit this corrosive aggressiveness. Therefore, this will depend on the carbonic acid content and the pH. The water's ability to corrode depends on the quantity of ions it contains. For example, near the city of Koudougou, a reddish color in the water has been observed, which led the population to abandon the wells. Studies conducted by [46, 60] in the Mouhoun basin in a sedimentary framework also showed this fact. The relationships of these orders of magnitude will depend on the relationships obtained [61–63].

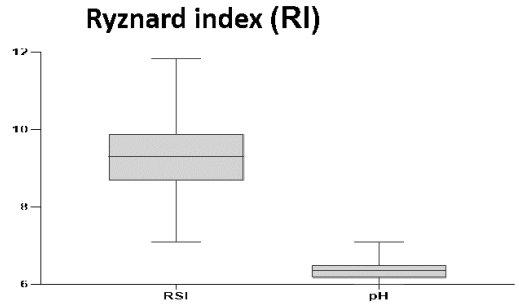

Figure 6. Statistical parameters of Ryznar indices.

3.2.3. Groundwater Characterization Using Principal Component Analysis

Eigenvalues/Variances: We begin by analyzing the eigenvalues using R. These eigenvalues also provide us with

the proportion of variance, that is, information retained by each principal component, which we extract using the appropriate function (**Table 3**).

In a second step, the Kaiser-Meyer-Olkin (KMO) test is applied to the sample. A high Kaiser-Meyer-Olkin index (usually > 0.5) indicates the relevance of PCA. Indeed, this method measures the adequacy of the data with the feasibility of PCA. The value found of 0.6 is largely satisfactory. The Bartlett test performed on the correlation matrix for the same eigenvalues verifies the suitability of the data. A chi-square value of 756.27 exceeds the critical value allowing for effective dimensional reduction. This demonstrates that PCA can effectively reduce the dimensionality of the original dataset. This reflects a perfect correlation of the variables for dimension reduction (**Table 3**).

The table is obtained as follows, for example, 3.132/10 equals 31.132, which is approximately 31.13% of the variation. The cumulative share of the variance gives us the cumulative percentage. For example, 31.13% plus 19.57% equals 50.70%. Consequently, approximately 72% of the total variance is found in the six values [52].

Furthermore, when CP > 1, it shows the accuracy of the information, thus ensuring dimensionality reduction, and (**Figure 7**) highlights the contribution of the variable.

Our study shows that the first six principal components contain 72% of all the information in the initial database (**Table 3**). This is a reasonable percentage considering that the initial database contained 16 variables. Another method to evaluate and verify the observed variance is to analyze the scree plot. Indeed, it represents the eigenvalues on the y-axis and the components on the x-axis (**Figure 7**).

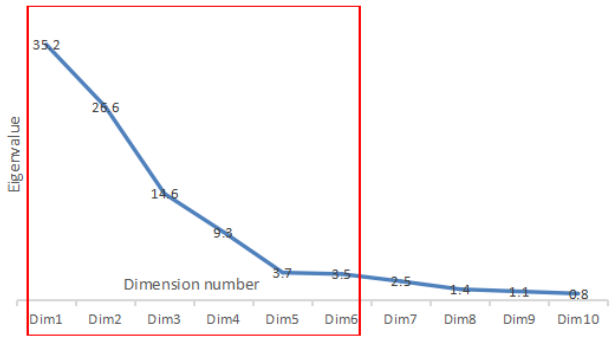

Figure 7. Drawing the collapse line for selecting major components.

The variable graph is represented in **Table 4**.

It is possible to visualize the variables and color them according to:

- their representational qualities (COS2) or
- their contributions to the main components (contrib).

Here, we examined the variables based on their graphical representation or their contribution to the CPs.

3.3. Correlation Circle

The relationship is used to define the position of the variable, as shown in **Figure 8**. This method of representing variables is distinct from the method used for observations, where variables are represented by their correlations with the principal components. Coloring according to cos2 indicates the quality of representation.

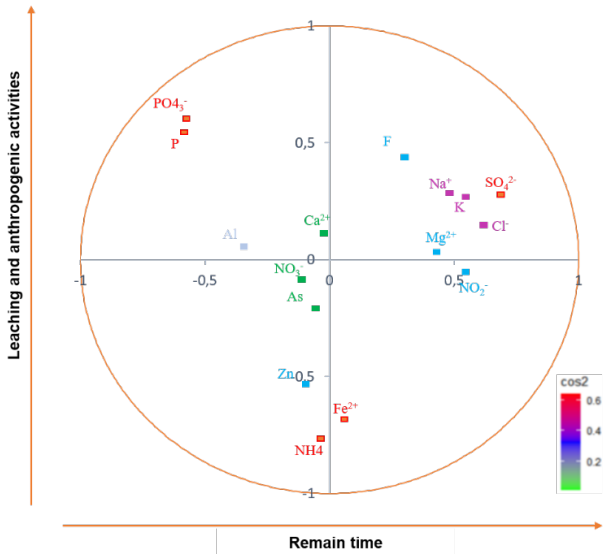

Figure 8. Quality of performance.

The quality of representation of variables on the PCA map is referred to as cos2 (square cosine) (**Figure 9**). We also endeavored to create a bar plot of the square cosine to better understand and analyze the variables.

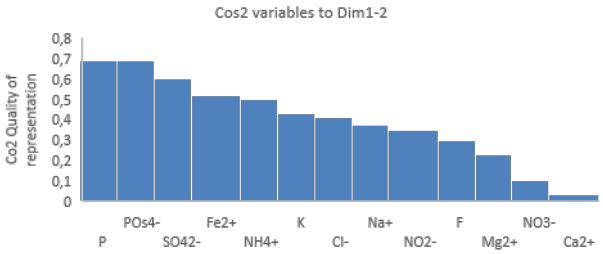

Figure 9. Bar plot of the square cosine of the variables.

Table 3. Cumulative variances and eigenvalues.

	Total	Variance (%)	Cumulative Variance (%)
Component 1	3.13^{e+00}	1.95^{e+01}	19.57
Component 2	2.47^{e+00}	1.54^{e+01}	35.02
Component 3	1.87^{e+00}	1.17^{e+01}	46.75
Component 4	1.55^{e+00}	9.69^{e+01}	56.45
Component 5	1.43^{e+00}	8.97^{e+01}	65.42
Component 6	1.17^{e+00}	7.33^{e+01}	72.76

Table 4. Results for active variables. (**a**) Quality of representation. (**b**) Contributions to major components.

	Principal Component Analysis Result for Individuals Name	Description
1	$"coord"	"Coordinates for the individuals"
2	$"coord"	"Cos2 for the individuals"
3	$"coord"	"Contributions of the individuals"

(a)

	Dim1	Dim2	Dim3	Dim4	Dim5
Ca^{2+}	5.55^{e-06}	0.01	0.50	0.13	2.63^{e-01}
Mg^{2+}	2.43^{e-01}	0.001	0.46	0.05	1.62^{e-01}
Na^{+}	3.03^{e-01}	0.07	0.07	0.005	2.65^{e-01}
K^{+}	3.26^{e-01}	0.06	0.0009	0.29	1.32^{e-01}
Fe^{2+}	4.39^{e-01}	0.52	0.04	0.04	6.94^{e-01}
Am	4.97^{e-01}	0.60	0.04	0.15	8.46^{e-05}

(b)

	Dim1	Dim2	Dim3	Dim4	Dim5
Ca^{2+}	1.77^{e-04}	0.66	26.94	8.44	18.38
Mg^{2+}	7.77^{e+00}	0.05	24/52	3.67	11.34
Na^{+}	9.69^{e+00}	3.03	4.10	0.34	18.48
K^{+}	1.04^{e+01}	2.61	0.05	19.04	9.22
Fe^{2+}	1.40^{e-01}	21.17	2.35	3.19	0.48
Am	1.58^{e-04}	24.41	2.23	9.87	0.005

We note:

A high squared cosine indicates an efficient representation on the main dimension analyzed. If it is close to the circumference, as shown by phosphorus, orthophosphate, sulfate, and ammonium, unlike nitrates, magnesium, and calcium. The summation of the axes represented by the squared cosines must eaual 1. The use of squared cosines confirms the reliability of the representation.

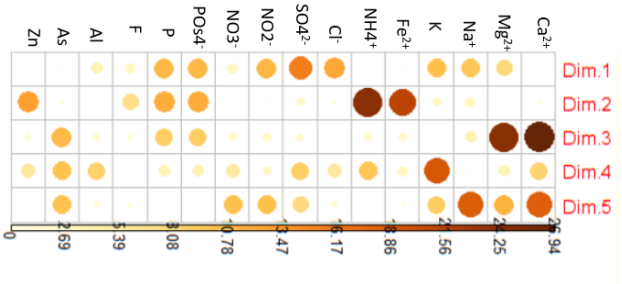

Figure 10. Value of the contribution.

3.3.1. Contributions of Variables to Main Axes

The following command allows us to see the contribution values (**Figure 10**). The two dimensions are crucial for expressing the confidence in the datasets as a percentage (**Table 5**). Data that are weakly correlated with these axes are not taken into account. The R code shows the top 5 variables that contribute the most to the principal components.

The most significant data are identified on the following graph (**Figure 11**).

3.3.2. Description of Dimensions

In the previous sections, the foregrounding of the data was determined based on their contribution to the principal components (**Tables 6** and **7**).

Table 5. Total contribution to FP1 and FP2.

	Dim1	Dim2	Dim3	Dim4	Dim5
Ca^{2+}	4.83	5.12	4.44	3.39	0.72
Mg^{2+}	0.03	0.09	0.02	0.22	0.26
Na^{+}	0.21	0.0009	0.06	0.10	0.03
K^{+}	0.05	0.38	0.03	0.12	1.20
Fe^{2+}	0.04	0.17	0.01	0.08	0.009
Am	0.26	0.01	0.13	0.004	0.20

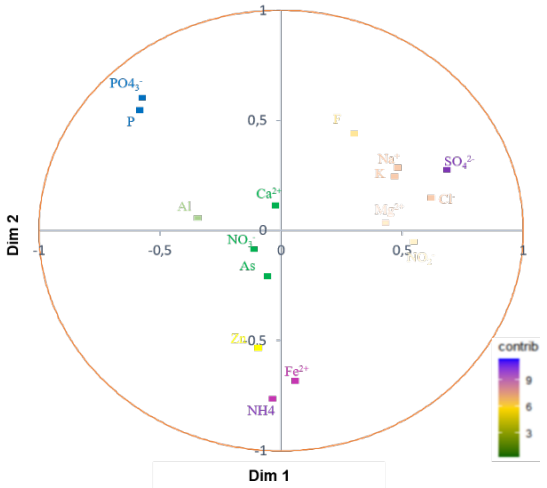

Figure 11. Correlation graph.

Table 6. Description de la dimension 1.

	Correlation	Value
SO_4^{2-}	0.70	4.50^{e-12}
Cl^{-}	0.61	4.05^{e-09}
NO_2^{-}	0.58	5.16^{e-08}
K	0.57	1.26^{e-07}
Na^{+}	0.55	4.36^{e-07}
Mg^{2+}	0.49	9.18^{e-06}
NO_3^{-}	0.31	6.46^{e-03}
F	0.30	8.91^{e-03}
Al	−0.36	1.42^{e-03}
P	−0.58	4.93^{e-08}
$POs4^{-}$	−0.58	4.93^{e-08}

Table 7. Description de la dimension 2.

	Correlation	Value
P	0.54	6.82^{e-07}
$POs4^{-}$	0.54	6.82^{e-07}
F	0.42	1.97^{e-04}
Na^{+}	0.27	1.89^{e-02}
K	0.25	2.99^{e-02}
SO_4^{2-}	0.24	3.57^{e-02}
Zn	−0.56	1.6^{e-07}
Fe^{2+}	−0.72	4.88^{e-13}
NH^{4+}	−0.77	6.71^{e-16}

The results presented above concern quantitative variables, sorted according to their correlation p-value.

3.3.3. Graph of Individuals

Figure 12 shows the matrix of individual results from the ‘get_pca_ind()‘ function [from the factoextra package]. Just like ‘*get_pca_var()‘, the ‘get_pca_ind()‘* function returns a list of matrices containing all the data.

To access the different elements, we went through the contact details of individuals through the *head(ind$coord) function,* then the quality of individuals through the *ead(ind$cos2) function.* Next, we checked the contribution of the individuals using the function (ind$contrib). This allowed us, in the end, to plot the graph of individual reliability.

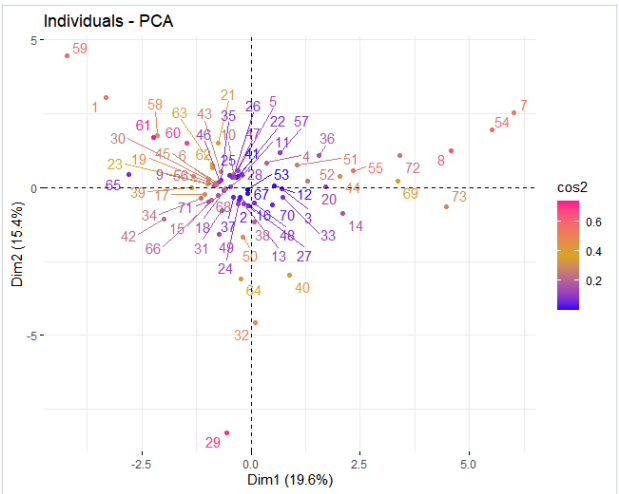

Figure 12. Graph of individuals.

3.3.4. Coloring by Groups and Ellipses of Concentration

We explain how to integrate confidence ellipses for specific groups (**Table 8**) and (**Figure 13**). To do this, we will use the iris dataset.

Table 8. Iris dataset.

	Sepal Length	Sepal Width	Petal Length	Petal Width	Species
1	5.1	3.5	1.4	0.2	setosa
2	4.9	3.0	1.4	0.2	setosa
3	4.7	3.2	1.3	0.2	setosa

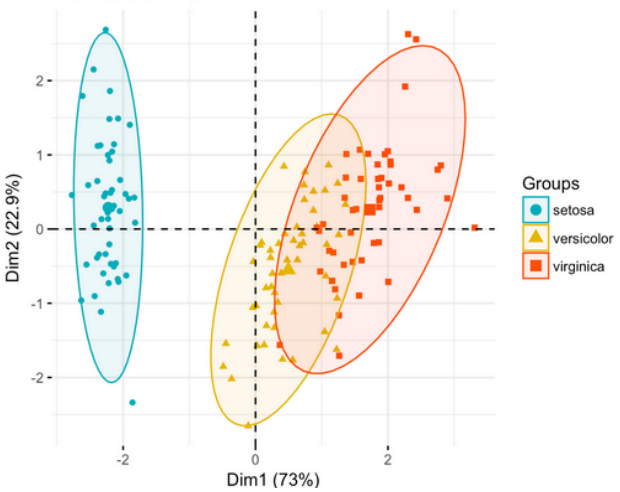

Figure 13. Ellipses of concentration.

If desired, it is possible to highlight concentration ellipses. So we also used ellipse.type = "confidence". We observe that the biplot becomes practical only when the dataset contains fewer individuals; otherwise, the final plot may become unreadable. Furthermore, the coordinates are not situated in the same center. Thus, our attention is more focused on their absolute position on the graph.

3.3.5. Discussion

Table 3 described in the section above shows the variance explained by each eigenvalue. Consequently, approximately 72% is explained by the first six eigenvalues. Indeed, it represents the eigenvalues (variance of the factors) on the ordinate axis (**Figure 7**).

The dimensions 1 to 5, represented by **Tables 4a** and **4b**, summarize the influence of the necessary variables. These constitute hydrochemical variables related to the mineralization of the geological complex and the constituent elements of soils. Each factor is characterized by a specific set of key variables to highlight the mechanism of mineralization and water pollution. We notice (**Tables 5** and **6**) that Dim1 represents 35% of the total variance and is influenced by variables such as Mg^{2+}, Na^{+}, Ca^{2+}, K^{+}, $SO_4{}^{2-}$, et Cl^{-}. hen Dim2 represents 26.6% of the total variance and is influenced by variables (**Table 5**) such as NH4, Fe^{2+}, Zn, $PO4_3{}^{-}$ and P. According to [46], this results from the rock expansion process leading to the alteration of the minerals in the parent rock, favoring the development of an alteration profile. Several factors affect this alteration, including the nature of the parent rock, the type of climate, the hydraulic gradient, the pH and temperature of the water, the biosphere, and the exposure time of the rock. The mineral concentration of water appears to be affected by the duration of residence, leading to leaching of rocks and potential chemical reactions within the aquifer [64–66]. Thirdly, Dim3 represents 14.6% of the total variance and is influenced by variables such as Mg^{2+}, Ca^{2+}, and As. According to Faye et al. [1], Bamba et al. [23] and Yameogo [48], leaching implies that undissolved elements remain in place or interact with other elements. Infiltration water, rich in CO_2, will attack plagioclase and biotite. Poorly crystallized compounds, silicate chains, and dissolved ions are transformed into new minerals, such as clays. However, the correlation matrix (**Table 2**) supports and corroborates these assertions.

Regarding the correlation circle (**Figure 8**) and the cos2 (**Figure 9**), it is observed that distinct groups have been identified. This is confirmed by the quality of the representation, which is indicated by the values of cos2. The variables will be colored based on their squared cosine levels: green for low values, blue for moderate values, and red for high values.

Therefore, based on the colour codes, we have a preliminary representation showing a positive correlation in red among the groups of ions NH_4, Fe^{2+}, Zn, $PO4_3{}^{-}$, P and $SO_4{}^{2-}$. This indicates an exchange from the soil, suggesting a strong contribution from anthropogenic activities. There is a lower correlation between As, NO_3- and Ca^{2+}. Indeed, this combination of ions indicates an anthropogenic contribution to water mineralization. Principal Component Analysis (PCA) revealed that two other factors contribute to water mineralization in the study area [67–69]. These are soil leaching and the influence of anthropogenic activities, with the lack of correlation between nitrate and zinc confirming this.

Still based on the color codes, we have the group of

ions Na^+, K^+ and Cl^-. There is a lower correlation between Mg^{2+}, F and $NO_2{}^-$. These indicators are typical of an environment where water interacts extensively with rock, thereby promoting prolonged dissolution time. Since hydrolysis is a gradual process, these conditions demonstrate how water chemistry evolves over time[70–72]. PCA confirms the presence of a negative relationship between contaminant compositions (major ions in this case) and pH, as well as a strong correlation between Ca^{2+} and $HCO_3{}^-$. The excess of $HCO_3{}^-$ in the water indicates that it comes from silicates and provides information about the residence time[73].

PCA applied to borehole samples reveals two principal axes. On one hand, there are positive correlations indicating a natural origin related to the petrography of the geological formation (silicates and their alteration products). On the other hand, negative correlations define the anthropogenic origin of mineralization linked to diffuse agricultural pollution. By projecting the points in the space of variables, we can infer that boreholes deviating from the cloud influenced by external inputs along the negative values of F2 are polluted. The boundary separating polluted from unpolluted waters is represented by the dashed vertical line. This indicates that the mineral sources are the same and pollution sources affecting boreholes first start affecting water from the shallow aquifer captured by wells. PCA analysis proves to be a relevant method in this context.

4. Conclusions

Previous studies have highlighted pollution across the 13 municipalities. However, nowadays, groundwater pollution has increased, leading to predictable health risks and the abandonment of some water points. The use of the saturation index and the implementation of PCA have improved the understanding of contamination. Average measurements indicate a predominantly acidic pH. Electrical conductivity readings suggest high mineralization, resulting in isolated water pockets. This level of mineralization and conductivity aligns perfectly with the deposition pattern, defined as the presentation and general organization of rocks in the subbasin. Indeed, in regions covered with lateritic duricrust, the duricrust aquifer is separated from the fractured rock aquifer. It is also noted that cations and anions increase with well depth. Additionally, while calcium and magnesium levels differ from one borehole, the opposite is true for chlorine and sodium. Bicarbonates make up the majority of the water's mineralization and outweigh other anions. These waters are also highly aggressive and corrosive throughout the basin, with the exception of the Yaké borehole in the To municipality. They also show saturation in calcite. Multivariate analyses have highlighted that mineralization is affected by soil leaching and human activities.

Author Contributions

Writing—original draft, validation, supervision, software, resources, project administration, methodology, investigation, data curation, conceptualization, M.D.F.; writing—review and editing, validation, software, resources, methodology, conceptualization, V.Y.B.L.; writing—review and editing, visualization, validation, methodology, A.K.; writing—review and editing, validation, M.D.; writing—review and editing, validation, funding acquisition, A.C.B.; writing—review and editing, validation, funding acquisition, M.K.; writing—review and editing, funding acquisition, H.Y.

Funding

The research received no external funding.

Institutional Review Board Statement

The study does not require ethical approval.

Informed Consent Statement

Not applicable.

Data Availability Statement

The authors agree to share their research data upon request.

Conflicts of Interest

The authors certify that there is no conflict of interest to declare.

References

[1] Faye, M.D., Loyara, V.Y.B., Biaou, A.C., et al., 2024. Modelling groundwater pollutant transfer mineral micropollutants in a multi-layered aquifer in Burkina Faso (West African Sahel). Heliyon. 10(1), e23557.

[2] Mounirou, L.A., Sawadogo, B., Yanogo, H., et al., 2023. Estimation of the actual specific consumption in drinking water supply systems in Burkina Faso (West Africa): Potential Implications for Infrastructure Sizing. Water. 15(19), 3423.

[3] Sawadogo, B., Faye, M.D., Konaté, Y., et al., 2023. Physico-chemical and microbial characterisation of water from the Abengourou dam in Eastern Côte d'Ivoire. American Journal of Environmental Protection. 12(4), 109–120.

[4] Clemenceau, B., 2018. What is the status of the human right to water and sanitation since the adoption of United Nations General Assembly Resolution No. 64/292 of 28 July 2010? The Review of Human Rights. Journal of the Centre for Research and Studies on Fundamental Rights. 13, 1–25.

[5] Unies, N., 2006. Report on the third session of the World Urban Forum. UN-HABITAT: Vancouver.

[6] Carter, R.C., Parker, A., 2009. Climate change, population trends and groundwater in Africa. Hydrological Sciences Journal. 54(4), 676–689.

[7] Mahamane, A.A., Guel, B., 2015. Physicochemical characterization of groundwater in the locality of Yamtenga (Burkina Faso). International Journal of Biological and Chemical Sciences. 9(1), 517–533.

[8] Paturel, J.-E., Boubacar, I., l'Aour, A., et al., 2010. Analyses of rainfall grids and main features of the changes that occurred in the 20th century in West and Central Africa. Hydrological Sciences Journal. 55(8), 1281–1288.

[9] Dewandel, B., 2019. Basement aquifers: Conceptual diagrams, pumping tests and regionalization of hydrodynamic properties [Ph.D. Thesis]. University of Montpellier: Montpellier, France. 97p.

[10] Faye, M.D., Biaou, A.C., Doulkom, P.A., et al., 2023. Contribution of remote sensing and geophysical prospecting (1D) to the knowledge of groundwater resources Burkina Faso. American Journal of Water Resources. 11(2), 2.

[11] Lachassagne, P., Wyns, R., 2005. Basement quiferous: New concepts. Application to prospecting and water resource management. Geosciences. 2, 32–37.

[12] Savadogo, N., 1984. Geology and hydrogeology of the crystalline basement of Upper Volta, Regional study of the Sissili watershed [Ph.D. Thesis]. Scientific and Medical University of Grenoble: Grenoble, France. 350p.

[13] Noronha, F., Cathelineau, M., Boiron, M.-C., et al., 2000. A three stage fluid flow model for Variscan gold metallogenesis in northern Portugal. Journal of Geochemical Exploration. 71, 209–224.

[14] Aboyeji, O.S., Eigbokhan, S.F., 2016. Evaluations of groundwater contamination by leachates around Olusosun open dumpsite in Lagos metropolis, southwest Nigeria. Journal of Environmental Management. 183, 333–341.

[15] Ikem, A., Osibanjo, O., Sridhar, M.K.C., et al., 2002. Evaluation of groundwater quality characteristics near two waste sites in Ibadan and Lagos, Nigeria. Water, Air, and Soil Pollution. 140(1–4), 307–333.

[16] Majolagbe, A.O., Adeyi, A.A., Osibanjo, O., et al., 2017. Pollution vulnerability and health risk assessment of groundwater around an engineering Landfill in Lagos, Nigeria. Chemistry International. 3(1), 58–68.

[17] Oluseyi, T., Adetunde, O., Amadi, E., 2014. Impact assessment of dumpsites on quality of near-by soil and underground water: A case study of an abandoned and a functional dumpsite in Lagos, Nigeria. International Journal Science Environment Technology. 3, 1004–1015.

[18] Osibanjo, O., Majolagbe, A.O., 2012. Physicochemical quality assessment of groundwater based on land use in Lagos city, southwest, Nigeria. Chemistry Journal. 2, 79–86.

[19] Penant, P., 2016. Characterization of nitrate sources in crystalline aquifers of central Benin [Ph.D. thesis]. University of Liège: Liège, Belgium. 97p.

[20] Lghoul, M., Maqsoud, A., Hakkou, R., et al., 2014. Hydrogeochemical behavior around the abandoned Kettara mine site, Morocco. Journal of Geochemical Exploration. 144, 456–467.

[21] Gandy, C.J., Younger, P.L., 2003. Effect of a Clay Cap on oxidation of Pyrite withinMine Spoil. Quarterly Journal of Engineering Geology and Hydrogeology. 36(3), 207–215.

[22] Bamba, O., Pelede, S., Sako, A., et al., 2013. Mapping of artisanal mining on the soils of a developed agricultural environment in Burkina Faso. Édité par Journal of Sciences. 13, 1–11.

[23] Faye, M.D., Kafando, M.B., Sawadogo, B., et al., 2022. Groundwater characteristics and quality in the cascades region of Burkina Faso. Resources. 11(7), 61.

[24] Keïta, A., Zorom, M., Faye, M.D., et al., 2023. Achieving real-world saturated hydraulic conductivity: Practical and theoretical findings from using an exponential one-phase decay model. Hydrology. 10(12), 235.

[25] Yameogo, A., Some, Y.S.C., Sirima, A.B., et al., 2020. Land use and soil erosion in the upper Sissili watershed, Burkina Faso. Africa Science. 17(5), 43–56.

[26] Ahoussi, E.K., Keumean, N.K., Kouassi, M.A., et al., 2017. Study of the hydrogeochemical and microbiological characteristics of drinking water in the peri-urban area of the city of Man: Case of the village of Kpangouin (Côte d'Ivoire). International Journal of Biologi-

cal and Chemical Sciences. 11(6), 3018–3033.

[27] Gil, M., Calvo, L., Blanco, D., et al., 2008. Evaluation of the agronomic aspects and environmental effects of the application of livestock manure compost to soil using multivariate methods. Bioresource Technology. 99, 5763–5772.

[28] Gournay, A., 2012. Multivariate Statistical Analysis [Lecture Notes].Université de Neuchâtel: Neuchâtel, Switzerland. 70p.

[29] Joliffe, I.T., 2002. Principal component analysis for special types of data. In: Joliffe, I.T. (Ed.). Principal Component Analysis. Springer: New York, NY, USA. pp. 338–372.

[30] Loyara, V.Y.B., Guillaume Bagré, R., Barro, D., 2020. Estimation of the Value at Risk Using the Stochastic Approach of Taylor Formula. International Journal of Mathematics and Mathematical Sciences. 2020, 6802932.

[31] Sass-Kiss, A., Kiss, J., Havadi, B., et al., 2008. Multivariate statistical analysis of botrytised wines of different origin. Food Chemistry. 110(3), 742–750.

[32] Silva, J.B.P., da Malvestiti, I., Hallwass, F., et al., 2005. Principal component analysis for verifying ^1H NMR spectral assignments: The case of 3-aryl (1, 2, 4)-oxadiazol-5-carbohydrazide benzylidenes. Química Nova. 28, 492–496.

[33] Soro, G., Soro, T.D., Adjiri, O.A., et al., 2019. Application of multivariate statistical methods to the hydrochemical study of groundwater in the Lake Region (central Ivory Coast). International Journal of Biological and Chemical Sciences. 13(3), 1870–1889. (in French)

[34] Cazes, P., Chouakria, A., Diday, E., et al., 1997. Extension of principal component analysis to interval data. Journal of Applied Statistics. 45(3), 5–24.

[35] Duby, C., Robin, S., 2006. Principal component analysis. National Agronomic Institute, Paris-Grignon: Paris. Volume 80, p. 53.

[36] Marques, W.S., Sial, A.N., de Albuquerque Menor, E., et al., 2008. Principal component analysis (PCA) and mineral associations of litoraneous facies of continental shelf carbonates from northeastern Brazil. Continental Shelf Research. 28(20), 2709–2717.

[37] Azevedo, D.A., Tamanqueira, J.B., Dias, J.C.M., et al., 2008. Multivariate statistical analysis of diamondoid and biomarker data from Brazilian basin oil samples. Fuel. 87(10–11), 2122–2130.

[38] Polat, K., Güneş, S., 2008. Artificial immune recognition system with fuzzy resource allocation mechanism classifier, principal component analysis and FFT method based new hybrid automated identification system for classification of EEG signals. Expert Systems with Applications. 34(3), 2039–2048.

[39] Harkat, M.-F., 2003. Detection and localization of defects by principal component analysis [Ph.D. Thesis]. Institut National Polytechnique de Lorraine-INPL: Nancy, France. 174p.

[40] Chaouki, I., Mouhir, L., Fekhaoui, M., et al. 2015. Application of principal component analysis (PCA) for the assessment of the quality of industrial wastewater from Salam Gaz–Skhirat. Journal of Materials and Environmental Science. 6(2), 455–464. (in French)

[41] Dahl, R., Hein K.A., Séjourné, S., et al., 2018. Geological, structural and mineral substances synthesis map of BURKINA FASO at a scale of 1:1,000,000, 60p.

[42] Giovenazzo, D., Séjourné, S., Hein K.A., et al., 2018. Explanatory note of the geological, structural and mineral substances synthesis map of BURKINA FASO at a scale of 1:1,000,000, 60p.

[43] Heriarivony, C., Razanamparany, B., Rakotomalala, J.E., 2015. Physico-chemical and bacteriological characteristics of drinking water (wells) in the rural commune of Antanifotsy, Vakinankaratra region, Madagascar. Larhyss Journal. 24, 7–17.

[44] Malik, N., Shimi, N.S., 2019. Study of the vulnerability of groundwater in the city of Gafsa (South-West Tunisia): Anthropogenic effects and consequences. Algerian Journal of Environmental Science and Technology. 5(4), 1127–1134.

[45] Merhabi, F., Amine, H., Halwani, J., 2019. Evaluation of the surface water quality of the Kadicha River. Lebanese Scientific Journal. 20(1), 10–34.

[46] Kouanda, B., Coulibaly, P., Niang, D., et al., 2018. Analysis of the performance of base flow separation methods using chemistry and statistics in Sudano-Sahelian watershed, Burkina Faso. Hydrology. Current Research. 9(2), 300.

[47] Saporta, G., 2006. Probabilities, data analysis, and statistics. Éditions Technip: Paris, France. 515p. (in French)

[48] Yameogo, S., 2008. Groundwater resources in the urban centre of Ouagadougou in Burkina Faso, quality and vulnerability. University of Avignon and Pays de Vaucluse [Ph.D. Thesis]. University of Ouagadougou: Avignon, France. 245p.

[49] Moussa, A.B., Zouari, K., Marc, V., 2011. Hydrochemical and isotope evidence of groundwater salinization processes on the coastal plain of Hammamet–Nabeul, north-eastern Tunisia. Physics and Chemistry of the Earth, Parts A/B/C. 36(5–6), 167–178.

[50] Faye, M., Biaou, A., Soro, D., et al., 2020. Understanding groundwater pollution of sissili catchment area in BURKINA-FASO. Larhyss Journal. 42, 121–144.

[51] Husson, F., Le, S., Pagès, J., 2017. Exploratory Multivariate Analysis by Example Using R. CRC press: Boca Raton, FL, USA.

[52] Kaiser, H.F., 1961. A note on Guttman's lower bound for the number of common factors. British Journal of Statistical Psychology. 14(1), 1–2.

[53] Peres-Neto, P.R., Jackson, D.A., Somers, K.M., 2005. How many principal components? Stopping rules

for determining the number of non-trivial axes revisited. Computational Statistics and Data Analysis. 49(4), 974–997.

[54] Abdi, H., Williams, L.J., 2010. Newman-Keuls test and Tukey test. Encyclopedia of Research Design. 2, 897–902.

[55] Husson, F., Lê, S., Pagès, J., 2011. Exploratory multivariate analysis by example using R. CRC press Boca Raton: Boca Raton, FL, USA. 244p.

[56] Bonifas, L., Escoufier, Y., Gonzalez, P.E., et al., 1984. Choice of variables in principal component analysis. Journal of Applied Statistics. 32(2), 5–15.

[57] Pagès, J., 2004. Mixed Data Factor Analysis. Journal of Applied Statistics. 52(4), 93–111.

[58] Savadogo, N., 1975. Hydrogeology of the Upper-Sissili watershed Upper Volta [Ph.D. Thesis]. Scientific and Medical University of Grenoble: Grenoble, France. 350p.

[59] Travi, Y., Dia, O., 1986. Hydrochemical interpretation on the basement formation aquifers of Eastern Senegal. 9p.

[60] Sauret, E., 2005. Hydrochemical characterization and groundwater quality of the village hydraulic project 310 boreholes in the Boucle du Mouhoun in the provinces of Banwa, Balés, Mouhoun and Kossi, Burkina Faso [Engineering Geologist Graduation]. Cheikh Anta Diop University: Dakar, Senegal. 63p.

[61] Ghazali, D., Zaid, A., 2013. Study of the physico-chemical and bacteriological quality of the waters of the Ain Salama-Jerri spring (Meknes-Morocco region). Larhyss Journal. 9782, 12.

[62] Hanon, M., Rouelle, A., 2011. The pH of the tap water. Environmental Portal of Wallonia: Belgium. 11p.

[63] Kahoul, M., Touhami, M., 2014. Evaluation of the physico-chemical quality of drinking water in the city of Annaba (Algeria). Larhyss Journal. 19, 129–138.

[64] Chenevoy, A., Piboule, M., 2017. Hydrothermalism. Metal hydric speciation and hydrothermal systems. Édition Diffusion Presse Sciences. 620p. (in French)

[65] Lachassagne, P., Wyns, R., Dewandel, B., 2011. The fracture permeability of hard rock aquifers is due neither to tectonics, nor to unloading, but to weathering processes. Terra Nova. 23(3), 145–161.

[66] Renac, C., Gal, F., Ménot, R.-P., et al., 2009. Mean recharge times and chemical modelling transfers from shallow groundwater to mineralized thermal waters at Montrond-les-Bains, Eastern Massif Central, France. Journal of Hydrology. 376(1), 1–15.

[67] Bian, J., Li, Y., Ma, Y., et al., 2022. Study on hydrochemical characteristics and formation process of antu mineral water in Changbai Mountain, China. Water. 14(18), 2770.

[68] Dechangue, T.R., Veronique, K.K., 2023. Use hydrochemistry and environmental isotopes for the assessment mineralization of groundwater in Miopliocene Aquifers in Douala 3 (Cameroon). American Journal of Water Resources. 11(1), 11–19.

[69] Gnamba, F., Baka, B., Sombo, A., et al., 2019. Quantitative and qualitative analysis of groundwater resources in the katiola region (côte d'ivoire). Larhyss Journal. 40, 117–134.

[70] Ahoussi, K.E., Koffi, Y.B., Kouassi, A.M., et al., 2012. Study of the chemical and microbiological characteristics of water resources in the N'zi watershed: Case of the commune of N'zianouan (South of Côte d'ivoire). International Journal of Biological and Chemical Sciences. 6(4), 1854–1873.

[71] Amadou, H., Laouali, M.S., Manzola, A., 2014. Physico-chemical and bacteriological analyses of the waters of three aquifers in the Tillabery region: Application of multivariate statistical analysis methods. Larhyss Journal. 20, 25–41.

[72] EBLIN, S., 2014. Degradation of environmental ecosystems in the Adiaké region (south-eastern coastal Côte d'ivoire) and risk of water pollution: Contribution of a SiG [Ph.D. Thesis]. FHB University, Abidjan: Bochum, Germany. 185p.

[73] Lasm, T., De Lasme, O., Oga, M.-S., et al., 2011. Hydrochemical characterization of fissured aquifers in the San-Pedro region (South-West Côte d'ivoire)). International Journal of Biological and Chemical Sciences. 5(2), 642–662.